

Scaling regimes for wormlike chains confined to cylindrical surfaces under tension

Greg Morrison^{1,2} and D. Thirumalai^{3,4}

1: Department of Physics, University of Houston, Houston TX 77204

2: Center for Theoretical Biological Physics, Rice University, Houston TX 77005

3: Departments of Chemistry, The University of Texas at Austin, Austin, TX, 78712

4: Department of Physics, The University of Texas at Austin, Austin, TX, 78712

August 29, 2023

Abstract

We compute the free energy of confinement \mathcal{F} for a wormlike chain (WLC), with persistence length l_p , that is confined to the surface of a cylinder of radius R under an external tension f using a mean field variational approach. For long chains, we analytically determine the behavior of the chain in a variety of regimes, which are demarcated by the interplay of l_p , the Odijk deflection length ($l_d = (R^2 l_p)^{1/3}$), and the Pincus length ($l_f = k_B T / f$, with $k_B T$ being the thermal energy). The theory accurately reproduces the Odijk scaling for strongly confined chains at $f = 0$, with $\mathcal{F} \sim L l_p^{-1/3} R^{-2/3}$. For moderate values of f , the Odijk scaling is discernible only when $l_p \gg R$ for strongly confined chains. Confinement does not significantly alter the scaling of the mean extension for sufficiently high tension. The theory is used to estimate unwrapping forces for DNA from nucleosomes.

1 Introduction

There are compelling reasons for understanding the static and dynamics of confined polymers because of their relevance in filtration, gel permeation chromatography, translocation of polymers and polypeptide chains through microporous membranes, and passage of newly synthesized proteins through the ribosome tunnel. These and other considerations prompted several theoretical studies, starting with pioneering studies [1, 2], which triggered subsequent theories and simulations that probed the fate of flexible polymers

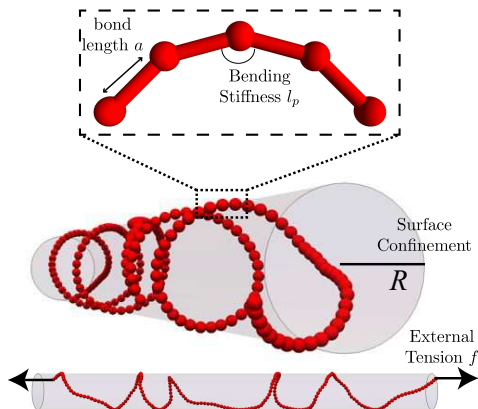


Figure 1: Schematic diagram of the chain backbone, with a fixed distance between monomers a and resistance to bending characterized by the persistence length l_p , the confinement to the surface of a cylinder of radius R , and an external tension f acting on the endpoints of the chain.

in pores with regular geometries [3, 4, 5, 6, 7, 8] as well as in the related case of random media [9, 10] is well understood.

The situation is somewhat more complicated when considering semi-flexible polymers or worm-like chains, WLC, in confined spaces. Spatial confinement of WLC plays an important role in many biological systems, such as, [11, 12, 13, 14, 15], including histone wrapping in chromatin [16, 17, 18, 19] and nanolithography [13, 20]. Here, we consider a WLC that is wrapped around a cylinder whose radius is R , and is subject to mechanical force (Fig. 1). Besides the total contour length (L), there are three length scales that control the statistics of the WLC polymer. The first is the persistence length l_p , which is a measure of the resistance of polymers to bending. For long unconfined chains the free energy is a function of l_p . In the mean field theory, proposed here, the polymer is globally restricted to be wound around the cylinder, which is equivalent to restraint enforced by a soft harmonic potential. Consequently, the Odijk length or the deflection length, $l_d = (R^2 l_p)^{1/3}$, emerges [21] coupling the chain stiffness and radius of confinement. In many biological contexts, the system is often under an external field elongating the chain, such as external tension (f) unravelling histone-wrapped DNA for replication [19]. An external tension or mechanical force is captured by the Pincus length [22], $l_f = (\beta f)^{-1}$ with $\beta = 1/k_B T$. The interplay of l_f , and l_p , and l_d on the conformations of the WLC is not fully

understood. The problem has some relevance to nucleosomes, consisting of DNA wrapped around histone proteins, which is a building block for chromosomes. Hence, the approximate theory developed here might illustrate an aspect of polymer theory in describing the physics of chromatin [11, 17].

In this paper, we propose a mean-field approach to study the properties of a wormlike chain confined to the surface of a cylinder [23] under the application of an external tension. Because l_p is comparable to the contour length, L , excluded volume interactions may be neglected. We recover the known [21, 24, 20, 25] dependence of free energy on the deflection length $l_d = (R^2 l_p)^{1/3}$ at $f = 0$. The theory predicts the coefficient of the leading term of the scaling of free energy, which is in good agreement with numerical results [23]. For moderate values of $f \neq 0$ (possibly relevant to DNA unwrapping from nucleosomes) and strong confinement ($l_p/R \gg 1$), we show that the free energy scales quadratically with l_f . At high external tensions, we find that the effect of confinement is perturbative, with $1 - \langle Z \rangle / L \sim \sqrt{l_f / l_p}$, independent of the radius of confinement.

2 Mean Field Theory

2.1 Formulation and approximations

In order to understand the equilibrium properties of a cylindrically confined WLC under tension, we developed a mean-field theory to arrive at analytically tractable results. The energy of a configuration of the chain is determined by a variety of terms that are sketched in Fig. 1. The system is characterized by the spacing between monomers (a), the number of bonds in the chain (the chain length $L = (N - 1)a \approx Na$ with $N \gg 1$), the persistence length of the unconfined chain (l_p), the confinement radius (R) aligned with the z -axis, and the external tension (f) that is also applied in the z direction. Let the position of each monomer be $\mathbf{r}_i = (x_i, y_i, z_i)$, and define $\mathbf{u}_i = \mathbf{r}_{i+1} - \mathbf{r}_i$ as the bond vector, and $\hat{\mathbf{u}}_i = \mathbf{u}_i / |\mathbf{u}_i|$ the unit bond vector. The statistics of a surface-confined chain can be described by a constrained Kratky-Porod (KP) Hamiltonian[26] $\beta H_{KP} = \frac{l_p}{a} \sum_{n=0}^N \hat{\mathbf{t}}_i \cdot \hat{\mathbf{t}}_{i+1} - \beta f (z_N - z_0)$, with confinement to the surface of the cylinder requiring $x_i^2 + y_i^2 = R^2$ for all i .

The KP model is mathematically difficult to work with because of two rigid constraints: the fixed bond length, $|\mathbf{u}_i| = a$, and the constraint that monomers be spatially constrained transverse to the z axis, which should

be enforced through the relation, $x_i^2 + y_i^2 = R^2$. On the mean field level, we replace these rigid constraints for the confined WLC with softer harmonic restraints (an approach that has been fruitfully applied previously [27, 25, 28, 29, 30]). The form of the MF Hamiltonian can be found by writing the monomer distribution function explicitly, in order to identify a physically meaningful harmonic approximation to the rigid constraints. It is straightforward to show that (up to a constant) the statistical weight is $\Psi_S = (\prod_{n=0}^N \delta[x_n^2 + y_n^2 - R^2]) \times (\prod_{n=1}^N \delta[|\Delta \mathbf{r}_n| - a]) \times (\prod_{n=1}^{N-2} e^{-l_p/2a^3(\Delta \mathbf{r}_{n+1} - \Delta \mathbf{r}_n)^2}) \times e^{+\beta f(z_L - z_0)}$ where $\Delta \mathbf{r} = \mathbf{r}_{n+1} - \mathbf{r}_n$ and $\beta = 1/k_B T$. The first term enforces confinement of the chain to the cylinder (affecting only the x and y coordinates of the polymer), the second term enforces the constant monomer spacing constraint, the third term accounts for the WLC's resistance to bending, and the fourth term accounts for the external tension. Each of the δ functions may be written as $\delta(x_n^2 + y_n^2 - R^2) \propto \int dk_n e^{iak_n[(x_n^2 + y_n^2)/R^2 - 1]}$ and $\delta(|\Delta \mathbf{r}| - a) \propto \int d\lambda_n e^{-ia\lambda_n[\Delta \mathbf{r}_n^2/a^2 - 1]}$, leading to,

$$\Psi_S \propto \int_{-i\infty}^{i\infty} \prod_n dk_n d\lambda_n \exp \left[-a \sum_{n=1}^N k_n \left(\frac{x_n^2 + y_n^2}{R^2} - 1 \right) - a \sum_{n=1}^{N-1} \lambda_n \left(\frac{\Delta \mathbf{r}_n^2}{a^2} - 1 \right) - \beta f(z_L - z_0) - \frac{1}{2} a \sum_{n=1}^{N-2} l_p \frac{(\Delta \mathbf{r}_{n+1} - \Delta \mathbf{r}_n)^2}{a^4} \right]. \quad (1)$$

The δ functions constrain enforce a fixed monomer separation and fixed transverse distance in the confined dimension. Here, we focus solely on surface confinement, but note that a MF approach has been applied to the confinement to the interior and surface [27] of a sphere. An equivalent volume constraint could be applied the interior of the cylinder through a constraint of $x_i^2 + y_i^2 \leq R^2$. However, a harmonic constraint on volume confinement requires an estimate of the average distance of each monomer in the transverse direction (which cannot be predicted at the mean field level).

Although exact, the formulation in Eq. 1 is difficult to work with directly. Analytical progress becomes possible by assuming that the integrals over the Fourier variables are sharply peaked, in the same manner as in our previous studies [27, 31]. The partition function $Z = \prod_n d^3 \mathbf{r}_n \Psi_S(\{\mathbf{r}_n\}) \equiv \int \prod_n d\lambda_n dk_n \exp(-\mathcal{F}[\{\lambda_n, k_n\}])$ defining the nondimensional free energy functional \mathcal{F} as an integral over all the monomer coordinates, and the linearity of the Fourier transform allows us to write $\mathcal{F} = \mathcal{F}_x + \mathcal{F}_y + \mathcal{F}_z - a \sum_{n=1}^N k_n - a \sum_{n=1}^{N-1} \lambda_n$, with $e^{-\mathcal{F}_x} \equiv \int \prod_n dx_n e^{-\mathcal{H}_c[\{x_n\}]}$ and $e^{-\mathcal{F}_z} \equiv \int \prod_n dz_n e^{-\mathcal{H}_u[\{z_n\}]}$,

where we define the confined Hamiltonian as, $\mathcal{H}_c[\{x_n\}] \equiv a \sum_{n=1}^{N-2} l_p (\Delta x_{n+1} - \Delta x_n)^2 / 2a^4 + a \sum_{n=1}^{N-1} \lambda_n \Delta x_n^2 / a^2 + a \sum_{n=1}^N k_n x_n^2 / R^2$. Similarly, the unconfined Hamiltonian is, $\mathcal{H}_u[\{z_n\}] \equiv a \sum_{n=1}^{N-2} l_p (\Delta z_{n+1} - \Delta z_n)^2 / 2a^4 + a \sum_{n=1}^{N-1} \lambda_n \Delta z_n^2 / a^2 + \beta f \sum_{n=1}^{N-1} \Delta z_n$. If the free energy is sharply peaked around some $\{\lambda_n, k_n\} = \{\lambda_n^*, k_n^*\}$ that minimizes \mathcal{F} , the partition function can be written approximately as $Z \approx Z^* = e^{-\mathcal{F}^*}$. Because the Hamiltonians \mathcal{H}_c and \mathcal{H}_u are uncoupled and quadratic in the monomer coordinates, it is straightforward to integrate over the internal coordinates of the polymer exactly. Along the confined axes, we find $\mathcal{F}_x = \mathcal{F}_y = \frac{1}{2} \log[\text{Det}(\mathbf{Q})]$, where the elements of the matrix $(\mathbf{Q})_{nm}$ are the coefficients associated with $x_n x_m$ in Eq. 2.1. The explicit form of $(\mathbf{Q})_{nm}$ is given in Appendix A of an earlier work [27]. In the unconfined direction, completing the square and noting the translational invariance of the system along the cylinder axis, allows us to write $\mathcal{F}_z = \frac{1}{2} \log[\text{Det}(\mathbf{P})] e^{\frac{1}{4}(\beta f)^2 a \sum_{n=1}^{N-1} \lambda_n^{-1}}$, with [31] $(\mathbf{P})_{ij} = \lambda_i \delta_{ij} - l_p \delta_{i,j \pm 1} / 2a^2$. These expressions can in principle be used to determine the stationary phase values for the Fourier variables by setting $\partial \mathcal{F} / \partial \lambda_n |_{\{\lambda_n, k_n\} = \{\lambda_n^*, k_n^*\}} = \partial \mathcal{F} / \partial k_n |_{\{\lambda_n, k_n\} = \{\lambda_n^*, k_n^*\}} = 0$. However, the resulting $2N - 1$ equations become intractable for large N , thus making it necessary to make additional approximations.

The matrices \mathbf{P} and \mathbf{Q} are bidiagonal and tridiagonal, respectively, with a regular structure except near the endpoints of the chain. The high symmetry of the matrices that underly the equations suggest that we should seek symmetric solutions for the stationary values of λ_n^* and k_n^* . In both the unconfined[31] and spherically confined[27] cases, it was shown that the tractable equations that reproduced exact theoretical results could be found for mean field parameters separated into bulk terms and endpoint terms[31, 27], with $\lambda_n^* = \lambda$ and $k_n = k$ for the interior points on the chain (those with $2 < n < N - 2$). Excess endpoint fluctuations generally require that $\lambda_1 = \lambda_{N-1} \neq 1$ and $k_1 = k_N \neq k \neq k_2 = k_{N-1}$ (with the equalities due to symmetry arguments). This approximation allows us to write $\mathcal{H}_c[\{x_n\}] = \mathcal{H}_c^{(b)}[\{x_n\}] + \mathcal{H}_c^{(e)}[\{x_n\}]$ and $\mathcal{H}_u[\{\Delta z_n\}] = \mathcal{H}_c^{(b)}[\{\Delta z_n\}] + \mathcal{H}_c^{(e)}[\{\Delta z_n\}]$, where the superscript b denotes an extensive bulk term, depending on the mean field parameters λ and k . The superscript e denoting an intensive endpoint term depending on the more complicated values of the mean field variables near the ends of the chain.

In the continuum limit, it can be shown that the bulk form of the Hamilto-

nians become,

$$\mathcal{H}_c^{(b)}[x(s)] = \int_0^L ds \left(\frac{l_p}{2} \ddot{x}^2(s) + \lambda \dot{x}^2(s) + k \frac{x^2(s)}{R^2} \right) \quad (2)$$

$$\mathcal{H}_u^{(b)}[z(s)] = \int_0^L ds \left(\frac{l_p}{2} \ddot{z}^2(s) + \lambda \dot{z}^2(s) - \beta f \dot{z}(s) \right). \quad (3)$$

The form for $\mathcal{H}_c^{(b)}$ is identical to the spherically confined Hamiltonian of the wormlike chain in our previous work [27], while the form of $\mathcal{H}_u^{(b)}$ is identical to that for an unconfined chain [31]. Note that λ is the same in the two Hamiltonians in Eq. 3 because of the condition $\langle \mathbf{u}^2 \rangle = \langle u_x^2 + u_y^2 + u_z^2 \rangle = 1$ couples the three components of the bending vector. However, the mean field parameter k occurs only in the confined Hamiltonian and enforces $\langle x^2 + y^2 \rangle = R^2$ constraint. The assumption that λ is isotropic causes inaccuracies in the predicted mean extension of a chain using the MF approach [32]. A MF theory that avoids this assumption has been developed [30], which does at the cost of greater complexity in the model. As we will show below, the expected scaling of the free energy in the limits of high tension and strong confinement are both recovered using an isotropic assumption, suggesting that the overall scaling laws will be accurate but with potentially inaccurate coefficients. We also ignore the endpoint effects by neglecting the Hamiltonians $\mathcal{H}_c^{(e)}$ and $\mathcal{H}_u^{(e)}$. This approximation simplifies the mathematics greatly, but restricts our analysis to very long chains. Neglecting the endpoint effects, the mean field equations for the extensive contribution to the free energy in the continuum are $\partial \mathcal{F} / \partial \lambda = \partial \mathcal{F} / \partial k = 0$, with $e^{-\mathcal{F}} = \int \mathcal{D}[\mathbf{r}(s)] e^{-\mathcal{H}_c^{(b)}[x(s)] - \mathcal{H}_c^{(b)}[y(s)] - \mathcal{H}_u^{(b)}[z(s)] + L(\lambda + k)}$.

2.2 Calculation of the Free Energy

It is straightforward to perform the path integrals over the confined [27] and unconfined [31] dimensions to explicitly compute the partition function $e^{-\mathcal{F}}$, from which it is possible to derive the mean field equations for constant λ and k . One can readily recognize that Eq. 3 describes a quantum harmonic oscillator after a change of variables, for which an exact propagator is known [33]. In the confined dimension, it is straightforward to show [27] that the action in Eq. 2 is minimized by a path satisfying $\frac{l_p}{2} x^{(4)}(s) - \lambda \ddot{x}(s) + \frac{k}{R^2} x(s) = 0$. It is readily observed (after some tedious mathematics) that the solution is expressible in terms of the frequencies $w_{\pm}^2 = \frac{\lambda}{l_p} (1 \pm \sqrt{1 - 2kl_p/\lambda^2 R^2})$. It is possible to integrate over the internal degrees of freedom of the chain exactly [27], which results in an unwieldy expression. However, with the

assumption that $\sinh(L\omega_{\pm}) \approx \cosh(L\omega_{\pm}) \approx e^{L\omega_{\pm}}/2$ (satisfied for $L/l_p \gg 1$), it is possible to simplify the confinement free energy as,

$$\frac{\mathcal{F}}{L} \approx \left(\omega_+ + \omega_- - k \right) + \left(\sqrt{\frac{\lambda}{2l_p}} - \lambda - \frac{(\beta f)^2}{4\lambda} \right), \quad (4)$$

where the first term is the contribution from integration over the chain configurations along the two confined axes, and the second is the contribution from the single unconfined axis. Endpoint effects are neglected in deriving Eq. 4, and is only valid for very long chains (where L is larger than all other length scales in the problem). The average extension of the chain, under tension, can be calculated using,

$$\langle Z \rangle = \frac{\partial \mathcal{F}}{\partial(\beta f)} = \frac{\beta f L}{2\lambda(l_p, R, f)}, \quad (5)$$

where we have explicitly included the dependence of the mean field solution of λ on the physical parameters at play. Eq. 5 is similar to the result found in the case of an unconfined chain under an external tension[28], which is straightforward to evaluate once the mean field solution for λ is known.

To determine the free energy and mean extension, we must solve the MF equations $\partial \mathcal{F} / \partial k = \partial \mathcal{F} / \partial \lambda = 0$. The resulting equations are greatly simplified by noting that

$$k = \frac{l_p R^2}{2} \omega_1^2 \omega_2^2 \quad \lambda = \frac{l_p}{2} (\omega_1^2 + \omega_2^2) \quad (6)$$

$$\frac{\partial \omega_{\pm}}{\partial \lambda} = \pm \frac{\omega_{\pm}}{l_p (\omega_+^2 - \omega_-^2)} \quad \frac{\partial \omega_{\pm}}{\partial k} = \mp \frac{1}{l_p R^2 \omega_{\pm} (\omega_+^2 - \omega_-^2)}. \quad (7)$$

After some algebra, the variational equations for λ and k , respectively, become

$$\frac{1}{l_p (\omega_+ + \omega_-)} = 1 - \frac{1}{\sqrt{8\lambda l_p}} - \frac{(\beta f)^2}{4\lambda^2} \quad \frac{1}{l_p (\omega_+ + \omega_-)} = R^2 \omega_+ \omega_-. \quad (8)$$

As the left-hand side of both equalities in the above equation are identical, we can readily solve for k in terms of λ , with,

$$k = \frac{l_p}{2R^2} \left(1 - \frac{1}{\sqrt{8\lambda l_p}} - \frac{1}{4} \left(\frac{\beta f}{\lambda} \right)^2 \right)^2 \quad (9)$$

so that the confinement parameter k at the mean field level can be determined exactly. The mean field parameter λ , enforcing the inextensibility of the chain, requires the solution of a complicated equation in Eq. 8, after substitution of the exact solution for k . Although it may not be possible to solve for the exact values analytically for all l_p , R , and f , it is straightforward to numerically determine the mean field values accurately for any l_p and R . The asymptotic behavior of the roots can be readily determined in certain limits, as discussed in the next section.

3 Results

3.1 Scaling for weak confinement and weak tension

An asymptotic solution to the Mean Field equations can be determined in a variety of parameter regimes. The simplest scenario is the limit where both the cylindrical confinement and the external tension are weak. In the limit of $R/l_f \ll 1$ (with $l_f = k_B T/f$ the Pincus length) and $l_p/R \ll 1$, the chain is weakly confined and we expect the mean field solution to be a perturbation on the solution to the unconfined three dimensional mean field theory. It has been shown [31] that $\lambda \sim 9/8l_p$ in the absence of external force or confinement. In order to determine the asymptotic behavior of the mean field parameter, we expand in a series for small values of the rescaled variables $\tilde{l}_p \equiv l_p/R \ll 1$ and $\varphi = R/l_f \ll 1$, with $\lambda R = \frac{9}{8l_p} + \sum_{m,n=0}^{\infty} b_{nm} \tilde{l}_p^n \varphi^m$ for some coefficients b_{nm} . Substitution for the exact solution for k in Eq. 9 into the MF equation for λ in eq. 8 allows us to perform a series expansion in higher order of \tilde{l}_p and φ , both assumed to be small. Iteratively solving for the lowest order coefficients b_{ij} shows $\lambda \approx \frac{9}{8l_p} - \frac{4l_p}{9R^2} + \frac{4l_p}{9l_f^2} + O(l_p^3/R^4)$, to leading order in \tilde{l}_p and φ . To leading order, the free energy under weak confinement and weak external tension is

$$\frac{\mathcal{F}}{L} \approx \frac{9}{8l_p} + \frac{2l_p}{9R^2} \left(1 - \frac{8l_p^2}{81R^2} \right) - \frac{2l_p}{3l_f^2} \quad (l_p \ll R, R/l_f \ll 1). \quad (10)$$

Note that retaining higher order terms in λ does not affect the scaling coefficients in eq. 10. It is interesting to note that the leading order contribution of the tension is independent of the radius of the cylinder, with the confinement only entering into the free energy through coupling with the persistence length. This is due to the distinct axes over which each energetic contribution acts, each of which are perturbative in this limit. Not surprisingly for weakly confined chains, the deflection length $l_d = (l_p R^2)^{1/3}$ does not enter

into the free energy. We note that these scaling coefficients are not likely to be precise, as has been previously noted for the MF solutions in multiple contexts [28, 30, 32]. However, the scaling with each variable is expected to be accurate.

For a weakly confined chain, the average extension in eq. 5 becomes

$$\frac{\langle Z \rangle}{L} \approx \frac{4}{9} \frac{l_p/l_f}{1 - 2 \left(\frac{4l_p}{9R} \right)^2}, \quad (11)$$

to fourth order in \tilde{l}_p and φ , growing linearly with f as long as $l_p \ll R$. The linear increase for low forces and weak confinement is shown in the purple triangles of Fig. 2 (A), satisfying the expected linear scaling.

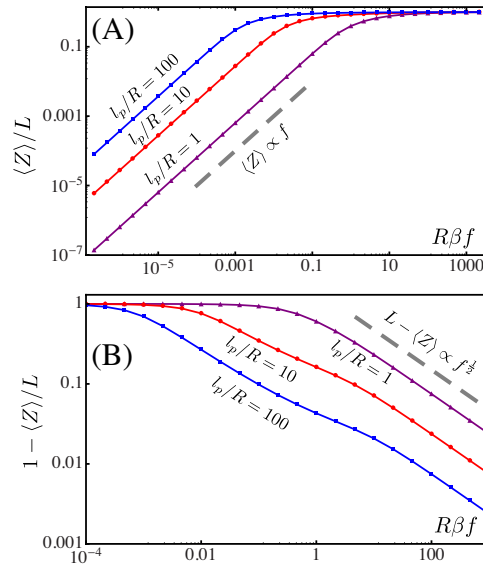


Figure 2: (A) Average chain extension (Eq. 5) as a function of f (with $R = 1$ held fixed) for various values of l_p : $l_p/R = 1$ (purple triangles), 10 (red circles), and 100 (blue squares). The extension increases linearly with force for small f , and the linear scaling is unperturbed by confinement effects. (B) The approach to full extension, $1 - \langle Z \rangle/L$, as a function of f scales as $f^{-1/2}$ for large external tension, but deviations from this scaling occur for very stiff chains.

3.2 Strongly confined chains under weak tension

It is also possible to determine the scaling behavior of the polymer under strong confinement (with $l_p \gg R$) but still constraining the external tension to be weak (with $R\beta f \ll 1$). A one-dimensional WLC in the absence of tension on the mean field level will satisfy $\lambda \sim 1/8l_p$, and we expect that λ must converge to this value for sufficiently small R or sufficiently large l_p (since transverse fluctuations must vanish in either limit). The effect of confinement is contained in the mean field variable k , which should capture the transverse statistics of the chain. It is known that the Odijk length scale, $l_d \propto (R^2 l_p)^{1/3}$, emerges for strongly confined WLCs to the interior of a cylinder [21, 25]. A stiff chain will predominantly be aligned with the cylinder axis, and l_d would be the typical distance along the chain for transverse fluctuations (a consequence of the mean field approach) to encounter the walls (causing a deflection). A similar scaling has been observed for surface confined chains [23] and we expect the deflection length to emerge at the MF level because the hard constraint is replaced by a soft harmonic potential. As a consequence, the stiff chain ‘deflects’ off the soft harmonic potential rather than a rigid wall.

In the limit of $\tilde{l}_p \equiv l_p/R \gg 1$ and $\varphi = R/l_f \ll 1$ we expect the leading order behavior of λ can be recovered with the ansatz $\lambda \approx \frac{1}{8l_p} + \sum_{n=4}^{\infty} c_n \tilde{l}_p^{-n/3} + \sum_{m=1}^{\infty} d_m \varphi^m$. This is similar to the expression for λ in the weakly confined case but with the expansion in terms of small φ and large $\tilde{l}_p^{1/3}$, and ignores cross-terms (assumed to be higher order, as was the case for weak confinement and low tension). The restriction of $n \geq 4$ in the sum over \tilde{l}_p ensures we recover the expected 1-d scaling for $R = 0$, since the leading order behavior is expected to be $\lambda = 1/8l_p$ for $R = 0$. Substitution into Eqs. 8 using 9 and taking the limit of small φ and large \tilde{l}_p shows that $c_4 = 0$ and $c_5 = 1/(4 \times 2^{1/3})$ cancel the lowest order terms in \tilde{l}_p , while $d_1 = 0$ and $d_2 = 4$ cancels the leading term in φ . Substitution of this solution into the free energy yields

$$\frac{\mathcal{F}}{L} \approx \frac{3}{2^{5/3}l_d} - \frac{2l_p}{l_f^2} + \frac{l_d}{l_f^2} + \frac{1}{8l_p}, \quad (12)$$

with the first term the leading order in the confinement, the second to leading order in l_f , the third term the lowest order coupling between the competing length scales l_d and l_f , and the fourth term the 1-dimensional MF free energy. In the absence of force, this expression for the free energy at a large external tension scales as L/l_d , agreeing with the known result for a

strongly confined WLC [21]. The coefficient of the leading term in Eq. 12 is $3/2^{5/3} \approx 0.945$, which will dominate in the limit of $R \rightarrow 0$. This compares reasonably well with the theoretical prediction for a surface-confined chain, with Eq. 38 in a previous study [23], which predicts a coefficient of 0.8416 by solving an exact nonlinear Fokker-Plank equation. We also note that the coefficient of the leading term of Eq. 12 is exactly twice the value Eq. [8] in an earlier report of DNA in confined to the interior of a cylinder [25]. This agreement along with the accurate prediction of the scaling coefficient in the previously studied case of spherical confinement using the mean field theory [27] suggest that even the calculated numerical coefficients arising may generally be reliable.

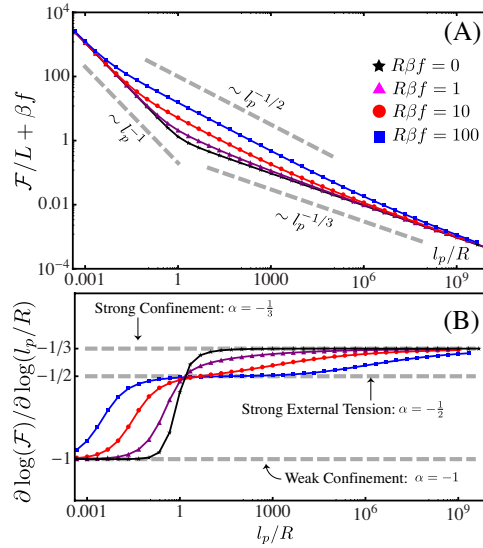


Figure 3: (A) Numerical roots for the extensive component of the mean field free energy for $R\beta f = 0$ (black stars), 1 (purple triangles), 10 (red circles), and 100 (blue squares) as l_p is varied and R held fixed. The scalings derived for the three asymptotic regimes are indicated by the gray dashed lines. The free energy is shifted by a factor L/l_f to counter the leading term in Eq. 15. (B) The coefficients α for the curves in (A) show that the scaling of $\mathcal{F} \sim l_p^{-1}$ and $\mathcal{F} \sim l_p^{-1/3}$ are recovered for sufficiently weak or sufficiently strong confinement respectively. Furthermore, $\mathcal{F} \sim l_p^{-1/2}$ is observed only for very large forces.

The scaling is confirmed by the numerical calculation for $l_p/R \gtrsim 10$ at $f = 0$

in the black stars in Fig. 3, and for non-zero forces the scaling is recovered for sufficiently strong confinement. Fig. 3(B) shows that non-zero tensions can significantly alter the onset of the Odijk regime. Even an external tension as low as, $R/l_f = 1$ (the purple triangles), delays the onset of the transition to the Odijk scaling, $\alpha = \partial \log(\mathcal{F})/\partial \log(l_p/R) = -\frac{1}{3}$, by orders of magnitude in l_p/R . In particular, we note that modeling the histone as a long cylinder of radius $R \approx 3.15\text{nm}$ and DNA with $l_p \approx 50\text{nm}$ will have a free energy of confinement satisfying the Odijk scaling at $f = 0$ (since $l_p/R \approx 16$). The binding of DNA to histones is known to be interrupted by forces on the order of $f \approx 10\text{pN}$ [19] and the unbinding of DNA already bound to histones occurs [19, 18] at forces $\approx 20 - 30\text{pN}$ (or $7.7 \lesssim \frac{R}{l_f} \lesssim 23.0$). The intermediate external tension in the red squares of Fig. 3 (with $R/l_f = 10$) falls within this range, indicating that the Odijk scaling may not be discernible by tensile forces over a wide range of biologically relevant conditions. It is interesting to note that confinement does not have a similarly strong affect on the scaling for the extension of a WLC under tension. The extension of the chain for small f and large l_p/R becomes

$$\frac{\langle Z \rangle}{L} \approx \frac{4l_p/l_f}{1 + \left(\frac{2R}{l_p}\right)^{2/3}}, \quad (13)$$

with the variations in the denominator being weak due to the approximation $l_p/R \gg 1$. Note that the scaling is linear in l_p , despite the emergence of the deflection length as the dominant length scale in the free energy in Eq. 12. We expect that even stiff chains will deviate only slightly from linear scaling (confirmed in the red squares and blue circles of Fig. 2(B)). The leading term in Eq. 13 differs from the extension of a weakly confined chain by a factor of $\frac{1}{9}$, which implies that strongly confined chains are expected to have a greater average extension at the same external tension as weakly confined chains (a physically sensible result). This is confirmed in Fig. 4, which shows that a decrease in the radius of the cylinder at fixed l_p , decreases the midpoint of extension (f_m , the force at which $\langle Z \rangle/L = 0.5$) from $l_p \beta f_m \sim 2$ by nearly an order of magnitude. For parameters matching the wrapping of DNA around a histone core, with $l_p \approx 16$ and $R \approx 3.15\text{nm}$, we predict that the midpoint of the transition is greatly reduced from its unconfined value, with $f_m(R \rightarrow \infty) \approx 0.16\text{pN}$ for the unconfined chain[28] and $f_m(R = 3.15) \approx 0.025\text{pN}$.

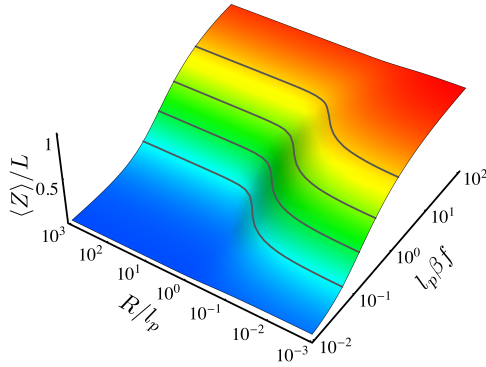


Figure 4: Extension $\langle Z \rangle / L$ for fixed $l_p = 1$ as R and f are varied. The midpoint of the force extension curve for sufficiently large $R/l_p \sim 10^3$ occurs near $l_p \beta f_m \sim 2$, but is reduced by nearly a factor of 8.8 for small $R/l_p \sim 10^{-3}$ to $l_p \beta f_m \sim 0.23$, in good agreement with the predicted reduction by a factor of 9 between weakly and strongly confined chains.

3.3 Confined chains under high tension

Finally, we consider the limit of external tensions that are strong enough to be comparable to confinement effects, satisfying $\frac{R}{l_f} \gtrsim l_p/R$. To determine the asymptotic form of the free energy in this limit, we define $\tilde{l}_p = l_p/R \equiv \sigma \times R/l_f = \sigma \varphi$ for some unconstrained σ (assumed finite, but not restricted to be large or small), and expand λ in the limit of large φ . In this limit, it is straightforward to show that $\lambda R \approx \frac{\varphi}{2} + \frac{3}{8\sqrt{\sigma}} + \frac{(9\sigma-8)}{32\sigma\varphi}$ to leading order in $\varphi \gg 1$. In the high-force and high-tension limit, the free energy becomes,

$$\frac{\mathcal{F}}{L} \approx -\frac{\varphi}{R} + \frac{3}{2R\sqrt{\sigma}} + \frac{1}{2R\varphi} \left(1 + \frac{9}{16\sigma}\right) \quad (14)$$

$$= -\beta f + \frac{3}{2} \sqrt{\frac{\beta f}{l_p}} + \frac{9}{32l_p} + \frac{1}{2\beta f R^2}. \quad (15)$$

Note that the free energy here does not depend on the deflection length $l_d \sim (l_p R^2)^{1/3}$ that was seen for strongly confined chains with low tension. Thus, a strong force significantly alter the free energy of confinement. The predicted scaling is confirmed in the blue circles in Fig. 3 for very large forces (with $R\beta f = 100$). We do not observe the expected limits of $\mathcal{F} \sim (l_p/l_f)^{-1/2}$ or $\mathcal{F} \sim (l_p R^2)^{-1/3}$ for strong confinement and intermediate tension (the purple triangles or red squares with $R/l_f = 1$ or 10 respectively), but instead

an extended crossover region between the expected scaling laws emerges. The average extension of the chain in this limit is similar to the unconfined WLC, with

$$\frac{\langle Z \rangle}{L} = 1 - \frac{3}{4\sqrt{l_p\beta f}}, \quad (16)$$

with the highest order dependence on the confinement radius scaling as $(\frac{R}{l_p})^{-2}$, which is assumed to be small in this limit. Note that the inextensibility of the chain is respected in the mean field theory (since $\langle Z \rangle \rightarrow L$ as $f \rightarrow \infty$), and that Eq. 16 (valid for sufficiently high forces) is identical to that of the unconfined chain. The approach to full extension is shown in Fig. 2(B), confirming the scaling of $1 - \langle Z \rangle / L \sim f^{-1/2}$ for large f regardless of the strength of confinement. Deviations from this scaling occur only for much weaker forces (with $l_p\beta f \lesssim 1$) for strongly confined chains.

4 Conclusions

In this paper, we calculated the free energy and linear extension of a worm-like chain confined to the surface of a cylinder with an applied external tension using a mean field approach. We conclude with the following additional comments. (1) Our method recovers the Odijk scaling of the free energy in the absence of force and the one-dimensional extension profile for a WLC in the limit of small cylinder radius. (2) The coefficient in Eq. 12 in the free energy expression obtained here is fairly close to the result obtained previously [23], which shows that the mean field theory not only predicts the scaling relation but also yields the coefficients that are fairly accurate. (3) For a nucleosome, $\frac{l_p}{R}$ lies in the range (5-10) depending on the concentration and valence of counter ions. Moreover, experiments [18] show that the first stage of DNA unwrapping occurs at $f \approx (3 - 5)$ pN. For these parameters, the theory predicts that $\alpha = \partial \log(\mathcal{F}) / \partial \log(l_p/R) \approx -0.5$ (red curve in Fig. 3B), which corresponds to strong external tension and modest confinement.

Acknowledgements: DT is grateful to Fyl Pincus for free lessons, with historical connotations, on polymer physics. This work was supported by grants from the National Science Foundation (CHE 2320256, PHY 2014141 and PHY 2019745) and the Welch Foundation through the Collie-Welch Chair (F-0019).

References

- [1] E.F. Casassa and Y Tagami. An equilibrium theory for exclusion chromatography of branched and linear polymer chains. *Macromolecules*, 2:14–26, 1969.
- [2] M Daoud and P.G. de Gennes. Statistics of macromolecular solutions trapped in small pores. *J. de. Physique*, 38:85–93, 1977.
- [3] F. Brochard-Wyart and E. Raphael. Scaling theory of molten polymers in small pore. *Macromolecules*, 23:2276–2280, 1990.
- [4] G. Morrison and D. Thirumalai. The shape of a flexible polymer in a cylindrical pore. *J. Chem. Phys.*, 122:194907, 2005.
- [5] S. Jun, D. Thirumalai, and BY Ha. Compression and stretching of a self-avoiding chain in cylindrical nanopores. *Phys. Rev. Lett*, 101:138101, 2008.
- [6] Cristian Micheletti, Davide Marenduzzo, and Enzo Orlandini. Polymers with spatial or topological constraints: Theoretical and computational results. *Physics Reports*, 504(1):1–73, 2011.
- [7] Youngkyun Jung, Chanil Jeon, Juin Kim, Hawoong Jeong, Suckjoon Jun, and Bae-Yeun Ha. Ring polymers as model bacterial chromosomes: confinement, chain topology, single chain statistics, and how they interact. *Soft Matter*, 8(7):2095–2102, 2012.
- [8] E Werner and B Mehlig. Confined polymers in the extended de gennes regime. *Physical review E*, 90(6):062602, 2014.
- [9] S. F. Edwards and D. Thirumalai. The size of a polymer in random media. *J. Chem. Phys.*, 89:2435–2441, 1988.
- [10] D. Thirumalai. Isolated polymer molecule in a random environment. *Phys. Rev. A*, 37:269–276, 1988.
- [11] Assaf Amitai and David Holcman. Polymer physics of nuclear organization and function. *Physics Reports*, 678:1–83, 2017.
- [12] Jeff ZY Chen. Theory of wormlike polymer chains in confinement. *Progress in Polymer Science*, 54:3–46, 2016.
- [13] Walter Reisner, Jonas N Pedersen, and Robert H Austin. DNA confinement in nanochannels: physics and biological applications. *Reports on progress in physics*, 75(10):106601, 2012.

- [14] Bae-Yeun Ha and Youngkyun Jung. Polymers under confinement: single polymers, how they interact, and as model chromosomes. *Soft Matter*, 11(12):2333–2352, 2015.
- [15] Omar A Saleh. Perspective: Single polymer mechanics across the force regimes. *The Journal of chemical physics*, 142(19), 2015.
- [16] J. Langowski. Polymer chain models of dna and chromatin. *Eur. Phys. J. E*, 19:241, 2006.
- [17] R. Everaers and H. Schiessel. The physics of chromatin. *J. Phys. Cond. Mat.*, 27:060301, 2015.
- [18] Y Cui and C Bustamante. Pulling a single chromatin fiber reveals the forces that maintain its higher-order structure. *Proc. Natl. Acad. Sci.*, 97:127, 2000.
- [19] M. L. Bennik, S. H. Leuba, G. H. Leno, J. Zlatanova, B. G. de Groot, and J. Greve. Unfolding individual nucleosomes by stretching single chromatin fibers with optical tweezers. *Nat. Struct. Biol.*, 8:606–610, 2001.
- [20] W. Reisner, K. J. Morton, R. Riehn, Y.M. Wang, Z. Yu, M. Rosen, J. C. Sturm, S. Y. Chou, E. Frey, and R. H. Austin. Statics and dynamics of single dna molecules confined in nanochannels. *Phys. Rev. Lett.*, 94:196101, 2005.
- [21] T. Odijk. On the statistics and dynamics of confined or entangled stiff polymers. *Macromolecules*, 16:1340, 1983.
- [22] P Pincus. Excluded volume effects and stretched polymer chains. *Macromolecules*, 9:386–388, 1976.
- [23] Y. Yang, T Burkhardt, and G. Gompper. Free energy and extension of a semiflexible polymer in cylindrical confining geometries. *Phys. Rev. E*, 76:011804, 2007.
- [24] M. Dijkstra, D. Frenkel, and H. NW Lekkerkerker. Confinement free energy of semiflexible polymers. *Physica A*, 193:374, 1993.
- [25] K. Jo, D.M Dalia, T Odijk, J. J. de Pablo, M. D. Graham, R Runnheim, D Forrest, and D. C. Schwartz. A single-molecule barcoding system using nanoslits for DNA analysis. *Proc. Natl. Acad. Sci.*, 104:2673, 2007.

- [26] M. Doi and S. F. Edwards. *The Theory of Polymer Dynamics*. Clarendon Press, Oxford, 1988.
- [27] G. Morrison and D. Thirumalai. Semiflexible chains in confine spaces. *Phys. Rev. E*, 79:011924, 2009.
- [28] BY Ha and D Thirumalai. Semiflexible chains under tension. *J. Chem. Phys.*, 106:4243, 1997.
- [29] J. Wang and H. Gao. Stretching a stiff polymer in a tube. *J. Mater. Sci.*, 42:8838–8843, 2007.
- [30] Greg Morrison. Correlation functions for strongly confined wormlike chains. <https://arxiv.org/abs/2003.12187>, 2023.
- [31] BY Ha and D. Thirumalai. A mean-field model for semiflexible chains. *J. Chem. Phys.*, 103:9408, 1995.
- [32] M Hinczewski and RR Netz. Anisotropic hydrodynamic mean-field theory for semiflexible polymers under tension. *Macromol*, 44:6972, 2011.
- [33] R. P. Feynman. *Statistical Mechanics*. W. A. Benjamin, Inc., 1982.